Metabolic Engineering 57 (2020) 193–202

Contents lists available at ScienceDirect

Metabolic Engineering

journal homepage: www.elsevier.com/locate/meteng

Metabolic engineering of *Escherichia coli* to produce a monophosphoryl lipid A adjuvant

Yuhyun Ji[a,b,1], Jinsu An[a,c,1], Dohyeon Hwang[a,c,1], Da Hui Ha[d], Sang Min Lim[c,e], Chankyu Lee[d], Jinshi Zhao[f], Hyun Kyu Song[b], Eun Gyeong Yang[a], Pei Zhou[f], Hak Suk Chung[a,c,*]

[a] Center for Theragnosis, Biomedical Research Institute, Korea Institute of Science and Technology, Seoul, Republic of Korea
[b] Department of Life Sciences, Korea University, Seoul, 02841, Republic of Korea
[c] Division of Bio-Medical Science & Technology, KIST School, Korea University of Science and Technology, Seoul, 02792, Republic of Korea
[d] Eubiologics.CO.,Ltd, V Plant 125, Wonmudong-gil, Dongsan-myeon, Chuncheon-si, Gangwon-do, Republic of Korea
[e] Convergence Research Center for Diagnosis, Treatment and Care System of Dementia, Korea Institute of Science and Technology, Seoul, Republic of Korea
[f] Department of Biochemistry, Duke University Medical Center, Durham, 27710, USA

ARTICLE INFO

Keywords:
Adjuvant
Monophosphoryl lipid A
Lipopolysaccharide biosynthesis
Gram-negative bacterial outer membrane
Lipid A 1-phosphatase
Vaccine adjuvant

ABSTRACT

Monophosphoryl lipid A (MPLA) species, including MPL (a trade name of GlaxoSmithKline) and GLA (a trade name of Immune Design, a subsidiary of Merck), are widely used as an adjuvant in vaccines, allergy drugs, and immunotherapy to boost the immune response. Even though MPLA is a derivative of lipopolysaccharide (LPS), a component of the outer membrane of Gram-negative bacteria, bacterial strains producing MPLA have not been found in nature nor engineered. In fact, MPLA generation involves expensive and laborious procedures based on synthetic routes or chemical transformation of precursors isolated from Gram-negative bacteria. Here, we report the engineering of an *Escherichia coli* strain for *in situ* production and accumulation of MPLA. Furthermore, we establish a succinct method for purifying MPLA from the engineered *E. coli* strain. We show that the purified MPLA (named EcML) stimulates the mouse immune system to generate antigen-specific IgG antibodies similarly to commercially available MPLA, but with a dramatically reduced manufacturing time and cost. Our system, employing the first engineered *E. coli* strain that directly produces the adjuvant EcML, could transform the current standard of industrial MPLA production.

1. Introduction

Lipid A (Fig. 1a) is a component of bacterial LPS, and it is a potent ligand for Toll-like receptor 4/myeloid differentiation 2 (TLR4/MD2) (Poltorak et al., 1998) as well as caspase-4, -5, and -11 (Shi et al., 2014; Hagar et al., 2013; Kayagaki et al., 2013). Lipid A (Fig. 1a), also known as the toxic component of endotoxin, can trigger excessive immune responses that result in septic shock (Lu et al., 2008); however, MPLAsm, which is chemically derived from *Salmonella* LPS (Fig. 1b and Supplementary Fig. 1), e.g., 3-O-desacyl-4′-monophosphoryl lipid A (MPL), and synthetic hexa-acylated MPLAs (MPLAsyn), e.g., GLA (also called PHAD) (Fig. 1c), PHAD-504, etc, have toxicity levels of only ~0.1% of that of LPS, but with comparable immune-stimulating activity (Casella and Mitchell, 2008). Owing to this property, MPL has been used as an adjuvant in human vaccines, including Cervarix, Fendrix, Mosquirix, and Shingrix (Reed et al., 2018), which are marketed by GSK. MPL was also proposed as a potential therapeutic option for Alzheimer's disease (Michaud et al., 2013). A synthetic hexa-acylated MPLA, GLA (Coler et al., 2011) (Fig. 1c), showed anticancer activity (Paya CuencaTer Meulen, 2015) and was developed by Immune Design as an orphan drug for follicular non-Hodgkin's lymphoma and soft tissue sarcoma. GLA and MPL have similar modes of action, targeting the TLR4/MD2 signaling pathway (Reed et al., 2016). MPL is typically prepared via acid/base hydrolysis of a precursor compound, Kdo_2-lipid A species, isolated from *S. minnesota* R549 (Qureshi et al., 1982) (Supplementary Fig. 1b). Since the resulting MPL has diverse congener compositions including hexa-, penta-, and tetra-MPL (Fig. 1b and Supplementary Fig. 1a), it is difficult to control the quality of the product. By contrast, synthetic GLA (Fig. 1c) is homogeneous, but its production requires multiple synthetic steps (Reed and Carter, 2014).

* Corresponding author. Center for Theragnosis, Biomedical Research Institute, Korea Institute of Science and Technology, Seoul, Republic of Korea.
E-mail address: hschung@kist.re.kr (H.S. Chung).
[1] These authors contributed equally to this work: Yuhyun Ji, Jinsu An, and Dohyeon Hwang

https://doi.org/10.1016/j.ymben.2019.11.009
Received 15 July 2019; Received in revised form 9 November 2019; Accepted 26 November 2019
Available online 28 November 2019

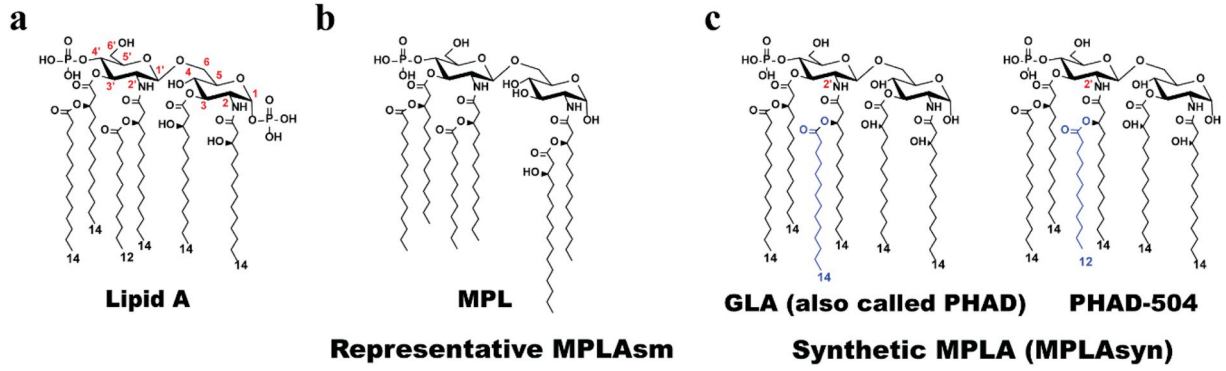

Fig. 1. Chemical structures of lipid A (the toxic component of endotoxin), MPLAsm, and MPLAsyn. (a) Lipid A structure. (b) A representative structure of MPLAsm (hexa-acylated MPL). Other MPLAsm structures are shown in Supplementary Fig. 1a. (c) Synthetic MPLA (GLA and PHAD-504) structures. PHAD-504 contains a lauroyl group (C_{12}) at the secondary acyl chain (blue colored fatty acid) of the 2′-position instead of a myristoyl group (C_{14}) compared with the GLA (PHAD) structure. (For interpretation of the references to color in this figure legend, the reader is referred to the Web version of this article.)

Given that MPLA is derived from lipid A, bacteria that could directly produce MPLA would offer tremendous value as a renewable resource along with simplified production steps to reduce production time and cost. Engineering a biosynthetic pathway for MPLA production in *E. coli* (Fig. 2, orange-colored box) is conceptually straightforward, but technically challenging, because the native LPS biosynthetic pathway has evolved to transfer Kdo sugars via the kdo transferase KdtA before incorporation of the secondary acyl chains by acyltransferases, i.e., lauroyltransferase (LpxL) and myristoyltransferase (LpxM) (Fig. 2, green-colored box). In wild-type *E. coli* cells, Kdo_2-lipid IV_A is first synthesized followed by Kdo_2-lipid A (Raetz and Whitfield, 2002), and MPLA is not produced. Therefore, to obtain MPLA, incorporation of the secondary acyl chains must occur in the absence of the Kdo_2 unit (Fig. 2, orange-colored box). Lipid A 1-phosphate phosphatase LpxE dephosphorylates the 1-phosphate of Kdo_2-lipid A or Kdo_2-lipid IV_A most efficiently (Supplementary Fig. 2) (Karbarz et al., 2009); however, it is not known whether any LpxE enzymes from Gram-negative bacteria can dephosphorylate lipid A substrates lacking the Kdo_2 sugar unit during outer membrane biogenesis. Moreover, prior to this study, it was thought that production of MPLA would be lethal for *E. coli* (Wang et al., 2015) since the minimum structure of LPS to support *E. coli* growth was reported as lipid IV_A that contains two phosphate groups (Mamat et al., 2008). This report describes an unprecedented *E. coli* strain that is bioengineered to produce MPLA directly without the need for additional hydrolysis and related purification processes.

2. Material and methods

The strains, plasmids, and primers used in this study are listed in Table 1 and Supplementary Table 1.

HPLC-grade chloroform and methanol and reagent-grade hydrochloric acid, sulfuric acid, aqueous ammonia, kanamycin, chloramphenicol, ammonium acetate, ampicillin, and LB broth were purchased from Merck (USA) or Sigma-Aldrich (USA), and Bacto agar was purchased from BD (USA). GLA (catalog no.: tlrl-mpls, lot: MPS-40-02; GLA and PHAD have the same chemical structure) and MPLAsm (catalog no.: tlrl-mpla, lot: MPL-38-02) were purchased from Invivogen (USA). Purified lipid A detoxified (from *Salmonella minnesota* R595, catalog no.: 699200P, lot: 699200P-1MG-A-031, MPLAsm), PHAD (catalog no.: 699800P, lot: 699800P-1MG-A-029), and PHAD-504 (catalog no.: 699810P, lot: 699810P-1MG-A-010) were obtained from Avanti Polar Lipids (USA). 1,2-dipalmitoyl-sn-glycero-3-phosphocholine was purchased from Sigma-Aldrich (USA, catalog no.: P0763) or Avanti Polar Lipids (USA, catalog no.: 850355). HRP-conjugated goat anti-mouse IgG (catalog no.: 1030–05), IgG1 (catalog no.: 1070–05), or IgG2a (catalog no.: 1080–05) antibodies were purchased from Southern Biotech (USA).

2.1. Plasmid construction

All primers were purchased from Macrogen (ROK). All polymerase chain reactions (PCRs) were performed using KOD Hot Start DNA Polymerase (Novagen, USA), PrimeSTAR HS (Takara, ROK), or Pfu polymerase (Elpisbio, ROK) in a T3000 Thermocycler (Biometra) or T100 Thermal Cycler (Bio-Rad). PCR products were purified using the DokDo-Prep PCR purification kit (Elpisbio, ROK) or the QlAquick PCR purification kit (Qiagen, USA). Plasmids were amplified in DH5α (Grant et al., 1990) cells and purified using the GeneJET plasmid Miniprep kit (Thermo Fisher Scientific, USA). The inserted genes in the plasmids constructed in this study were sequenced by Macrogen (ROK).

The $lpxE_{HP}$ (*hp0021*) gene was synthesized by IDT (USA) with a silent mutation at Ser17 (from AGC to TCG) to remove a *Hin*dIII recognition site and amplified with the $LpxE_{HP}$-5′ and $LpxE_{HP}$-3′ primer pair. The $lpxE_{AA}$ (*aq_1706*) gene was amplified using the $LpxE_{AA}$-5′ and $LpxE_{AA}$-3′ primer pair with pET21-AaLpxE (Zhao et al., 2019) as the template. The $lpxE_{FN}$ and $lpxE_{RL}$ genes were amplified using Primer pairs: $LpxE_{FN}$-5′ and $LpxE_{FN}$-3′ and $LpxE_{RL}$-5′ and $LpxE_{RL}$-3′ with pET28b-FnLpxE (Wang et al., 2004) and pLpxE-4 (Karbarz et al., 2009) as templates, respectively. The *lpxE* genes were inserted individually into pBAD33.1 (Chung and Raetz, 2010) using *Xba*I and *Hin*dIII restriction enzyme recognition sites. To construct the pWSK29-$lpxL_{EC}lpxM_{EC}$ plasmid, two sequential PCRs were performed. First, the $lpxL_{EC}$ and $lpxM_{EC}$ genes were amplified with two primer pairs, LpxL-5′ and LpxL-3′ and LpxM-5′ and LpxM-3′, respectively, and the fragments were then fused to generate the $lpxL_{EC}lpxM_{EC}$ fragment via extended PCR using the LpxL-5′ and LpxM-3′ primers and the PCR products from the first PCR reactions as the template. The resulting $lpxL_{EC}lpxM_{EC}$ fragment was inserted into pWSK29 (Wang and Kushner, 1991) using the *Xba*I and *Hin*dIII restriction enzyme recognition sites.

2.2. Construction of KHSC0003/pBAD33.1, KHSC0003/pBAD33.1-$lpxE_{AA}$, and KHSC0003/pBAD33.1-$lpxE_{HP}$ (Fig. 3a and 3b)

P1*vir* generation and P1 transduction were performed following a previously described procedure (Thomason et al., 2007). The kanamycin-resistance (kan^R) cassette was removed from the W3110 chromosome using pCP20 according to the previously published procedure (Datsenko and Wanner, 2000).

A *lpxT::kan* knockout mutation was transduced into W3110 via P1*vir* grown on JW2162 (*lpxT::kan*) (Baba et al., 2006), and the kan^R cassette was removed via pCP20. The *pagP::kan* mutation was transduced into the Δ*lpxT* W3110 strain with P1*vir* grown on JW0617, and the kan^R cassette was then removed. The resulting strain was named KHSC0001 (Δ*lpxT* Δ*pagP* W3110). To construct KHSC0003, pWSK29-$lpxL_{EC}lpxM_{EC}$ was transformed into KHSC0001 and *kdtA* was then

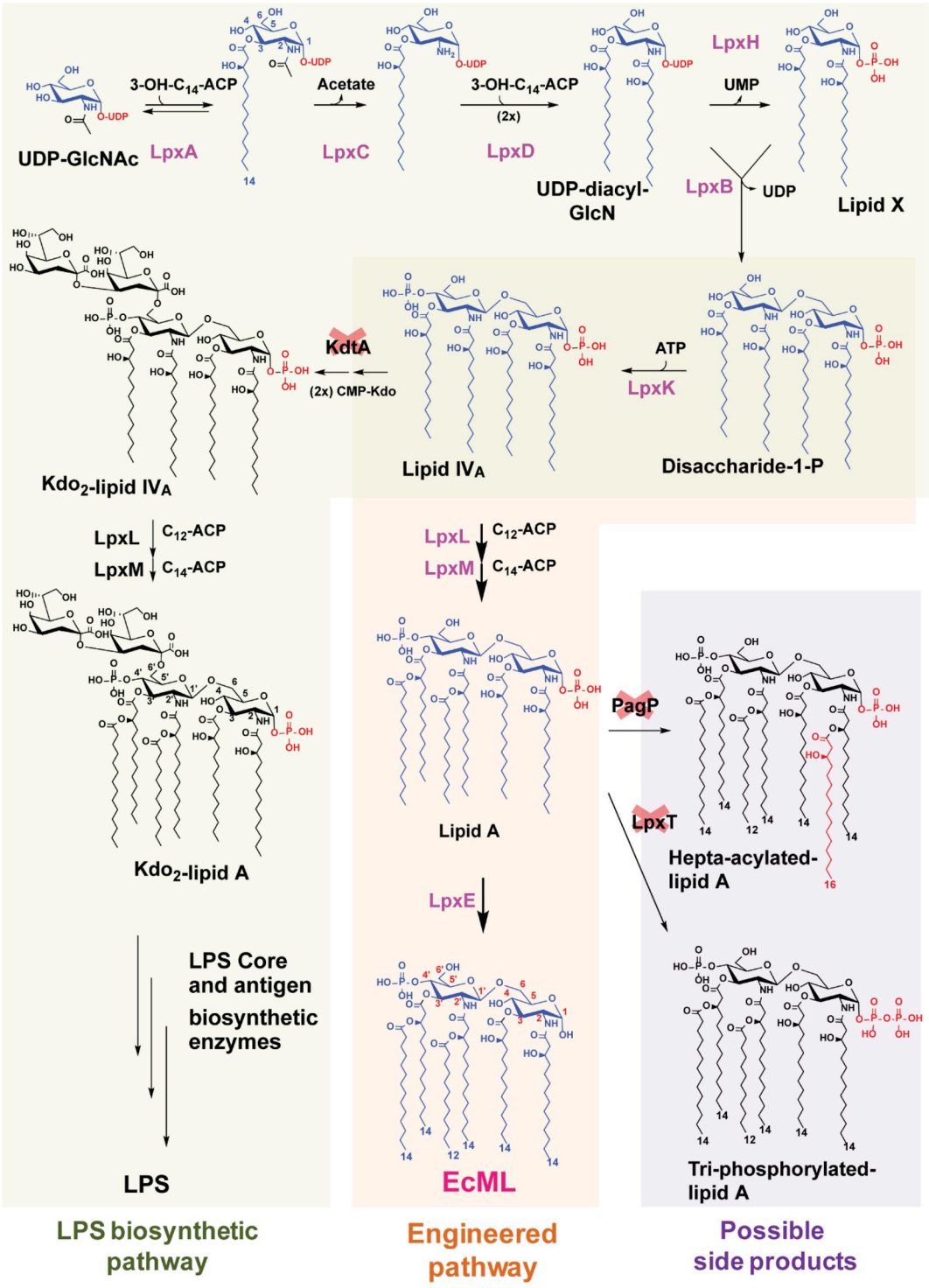

Fig. 2. The proposed *de novo* biosynthetic pathway for MPLA production. LPS biosynthesis and the proposed *de novo* biosynthetic pathway for MPLA. *E. coli* evolved to incorporate Kdo sugar units via Kdo transferase KdtA before addition of the lauroyl and myristoyl groups by LpxL and LpxM, respectively, during LPS biogenesis (green-colored box). A proposed MPLA biosynthetic pathway in *E. coli* is shown in the orange-colored box (blue-colored pathway). Red crosses indicate the necessary gene knockouts for generating the MPLA-producing strains. LpxT and PagP potentially compete with LpxE for lipid A as a substrate (purple-colored box). (For interpretation of the references to color in this figure legend, the reader is referred to the Web version of this article.)

knocked out via P1*vir* grown on HSC1/pEckdtA (Chung and Raetz, 2010) in the presence of 1 mM isopropyl β-D-1-thiogalactopyranoside (IPTG).

The pBAD33.1, pBAD33.1-$lpxE_{AA}$, and pBAD33.1-$lpxE_{HP}$ plasmids were transformed singly into KHSC0003 via electroporation (Seidman et al., 1997), and the transformants were selected on LB agar plates containing 1 mM IPTG, 100 μg/mL ampicillin, and 30 μg/mL chloramphenicol. The chromosomal knockouts of *lpxT*, *pagP*, and *kdtA* were confirmed by PCR using the primer pairs lpxT-up/lpxT-down, pagP-up/pagP-down, and kdtA-up/kdtA-down, respectively (Supplementary Fig. 3b). Genomic DNA was isolated from KHSC0003/pBAD33.1-$lpxE_{AA}$ using QIAamp genomic DNA kits (Qiagen, USA). *De novo* sequencing of KHSC0003/pBAD33.1-$lpxE_{AA}$ genome and analyses for single nucleotide polymorphism (SNP)s and indels in comparison

Table 1
Strains and plasmids used in this study.

Strain	Relevant properties	Source or reference
W3110	Wild type F^- λ^- *rph-1 IN(rrnD, rrnE)*	*E. coli* Genetic Stock Center, Yale
C41(DE3)	F^- *ompT* $hsdS_B$ ($r_B^-m_B^-$) *gal dcm* (DE3)	Miroux and Walker (1996)
DH5α	F- ϕ80*lacZ*ΔM15 Δ(*lacZYA-argF*)U169 *recA*1 *endA*1 *hsdR*17(rk^-, mk^+) *pho*A *sup*E44 *thi*-1 *gyr*A96 *rel*A1 λ^-	Grant et al. (1990)
JW2162	*lpxT::kan* BW25113	Baba et al. (2006)
JW0617	*pagP::kan* BW25113	Baba et al. (2006)
HSC1/pEcKdtA	*kdtA::kan* DY330/pEcKdtA	Chung and Raetz (2010)
KIHSC001	*lpxT::kan* W3110	This work
KIHSC002	Δ*lpxT* W3110	This work
KIHSC003	Δ*lpxT pgpP::kan* W3110	This work
KHSC0001	Δ*lpxT* Δ*pagP* W3110	This work
KHSC0001-1	KHSC0001/pWSK29-$lpxL_{EC}lpxM_{EC}$	This work
KHSC0003	*kdtA::kan* KHSC0001-1	This work
KHSC0003-1	KHSC0003/pBAD33.1	This work
KHSC0003-2	KHSC0003/pBAD33.1-$lpxE_{AA}$	This work
KHSC0003-3	KHSC0003/pBAD33.1-$lpxE_{HP}$	This work
KHSC0003-4	KHSC0003/pBAD33.1-$lpxE_{FN}$	This work
KHSC0003-5	KHSC0003/pBAD33.1-$lpxE_{RL}$	This work
Plasmid	**Relevant properties**	**Reference**
pWSK29	Low copy vector, lac promoter, Amp^R	Wang and Kushner (1991)
pWSK29-$lpxL_{EC}lpxM_{EC}$	pWSK29 harboring *E. coli lpxL* and *lpxM*	This work
pET21a-$lpxE_{AA}$	pET21a harboring *A. aeolicus lpxE* (*aq_1706*)	Zhao et al. (2019)
pBAD33.1	Medium copy vector, Cam^R	Chung and Raetz (2010)
pBAD33.1-$lpxE_{AA}$	pBAD33.1 harboring *A. aeolicus lpxE* (*aq_1706*)	This work
pBAD33.1-$lpxE_{HP}$	pBAD33.1 harboring *H. pyroli* $lpxE_{HP}$ (*hp0021*)	This work

with the published W3110 genome (Genebank accession number AP009048) were done by Macrogen (ROK). The identified SNPs and indels were compared to the sequence of PCR products amplified from W3110 genome used for KHSC0003/pBAD33.1-$lpxE_{AA}$ construction.

2.3. Growth conditions of strains and lipid extraction from cell pellets

Growth curve: W3110 and KHSC0001 in LB broth (Miller) (Merck 1.10285.5000) medium, KHSC0001-1 in LB broth medium supplemented with ampicillin (100 μg/mL), KHSC0003 in LB broth medium

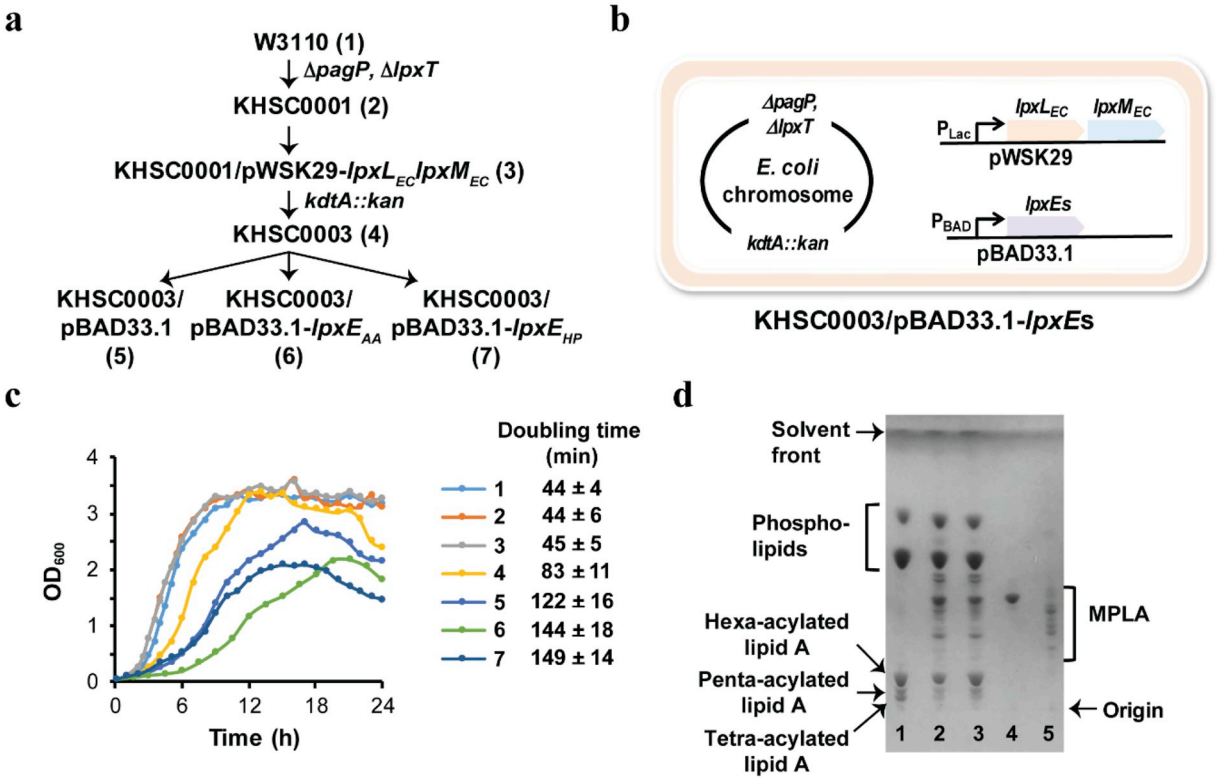

Fig. 3. Engineered *E. coli* strains that directly produce MPLA. (a) Schematic illustration of the construction of the MPLA-producing *E. coli* strain KHSC0003/pBAD33.1-*lpxEs*. (b) Schematic diagram of the MPLA-producing strain. (c) Growth curves for all engineered strains and the mother strain W3110. The number 1–7 correspond to the strains shown on panel (a). (d) TLC profiles of the lipids extracted from the engineered *E. coli* strains compared to those of GLA (lane 4) and MPLAsm (lane 5). Total lipids extracted from KHSC0003/pBAD33.1 (lane 1), KHSC0003/pBAD33.1-$lpxE_{AA}$ (lane 2), and KHSC0003/pBAD33.1-$lpxE_{HP}$ (lane 3).

supplemented with ampicillin (100 μg/mL) and 1 mM IPTG, and KHSC0003/pBAD33.1, KHSC0003/pBAD33.1-*lpxE*$_{AA}$, and KHSC0003/pBAD33.1-*lpxE*$_{HP}$ in LB broth medium supplemented with ampicillin (100 μg/mL) and chloramphenicol (30 μg/mL), and 1 mM IPTG were grown at 30 °C with shaking (180 rpm) for 24 h. Then cultures were diluted (OD_{600} ~ 0.05) into 300–500 mL of LB medium with the same supplements. After 12 h of growth, KHSC0003, KHSC0003/pBAD33.1, KHSC0003/pBAD33.1-*lpxE*$_{AA}$, and KHSC0003/pBAD33.1-*lpxE*$_{HP}$ were supplemented with 1 mM IPTG and incubated at 30 °C with shaking (180 rpm). Doubling time was calculated using the equation (doubling time = ln2/r where r = (ln OD_2 – ln OD_1)/(t_2-t_1)) based on the growth curve (OD_{600} range from ~0.2 to 1.2 for each strain).

IPTG effect on the growth and the MPLA production of KHSC0003/pBAD33.1-*lpxE*$_{AA}$: The seeding culture was diluted into LB medium in the presence of ampicillin (100 μg/mL) and chloramphenicol (30 μg/mL) with 0 or 1 mM IPTG. After 12 h of growth, 0 or 1 mM IPTG was added into the culture.

L-arabinose (Ara) effect on the growth and the MPLA production of KHSC0003/pBAD33.1-*lpxE*$_{AA}$: The seeding culture was diluted into the LB broth medium containing ampicillin (100 μg/mL), chloramphenicol (30 μg/mL) and 1 mM IPTG in the presence of 0, 0.01, 0.1, or 1 mM arabinose and 1 mM IPTG was added into the culture at 12 h after inoculation.

Lipid extraction: After 22–28 h growth, cells were harvested via centrifugation at 2900 RPM (1,777 g, Hanil s500 4B rotor, Centrifuge COMBI-514R, Hanil Science Industrial Co., Ltd.) for 1 h or centrifugation at 8,000 g for 15 min at 4 °C, and the resulting pellets were washed with deionized water or phosphate-buffered saline (PBS). Lipids were extracted from the pellets via the Bligh-Dyer system (Bligh and Dyer, 1959) and analyzed via thin-layer chromatography (TLC) in a solvent system consisting of a chloroform/methanol/water/ammonium hydroxide solution (40:25:4:2 v/v).

2.4. Purification and characterization of EcML

The extracted lipids were fractionated via ion-exchange chromatography using a DEAE cellulose column (IonSep DE52 Cellulose Preswollen, Biophoretics) (Raetz et al., 1985) with increasing ammonium acetate concentrations following the procedure described for phosphatidylglycerol phosphate fractionation (Lu et al., 2011). Fractions containing EcML were converted to a two-phase Bligh-Dyer system by adding appropriate amounts of water and chloroform. The lower organic phase was evaporated under a stream of N_2 (g). EcML was analyzed in comparison with GLA and MPLAsm via TLC. The TLC plates were visualized by spraying 10% (v/v) sulfuric acid (in ethanol) followed by charring on a hot plate at 300 °C. The purity of EcML was assessed via the TLC and ESI-MS methods and determined based on TLC images using the ImageJ software (Schneider et al., 2012). Quantification of EcML was determined by weighing samples using an analytical balance with a precision of 0.1 mg.

2.5. MALDI-TOF, ESI-MS, and HPLC analysis of lipids

Total lipids were dissolved in chloroform and methanol at a ratio of 4:1 (v/v). The resuspended lipid samples were loaded on a matrix consisting of 10 mg/mL 2,5-dihydroxybenzoic acid solution (Sigma-Aldrich) and acetonitrile (Sigma-Aldrich) at a ratio of 1:4 and then analyzed using a MALDI-TOF mass spectrometer (Shimadzu Biotech Axima Resonance) at Korea Basic Science Institute. The mass spectra were analyzed via the mMass software (http://www.mmass.org/).

EcML was dissolved in chloroform and methanol at a ratio of 4:1 (v/v) at a concentration of 1 mg/mL and then diluted with 4:1 (v/v) chloroform:methanol solution at a 1:400 ratio. The sample was analyzed via ESI-MS (TSQ Quantum Ultra EMR) at Korea Basic Science Institute. For the congener analysis, EcML, GLA, MPLAsm, MPLAsyn, and PHAD-504 were derivatized with dinitrobenzyloxyamine (DNBA, Sigma-Aldrich) and analyzed via HPLC chromatography (Prominence, Shimadzu) as described previously (Hagen et al., 1997).

2.6. Mouse immunization

All animal experiments were performed via protocols approved by the Institutional Animal Care and Use Committee (IACUC) of Chuncheon Bioindustry Foundation. Aqueous formulations of EcML, GLA, and MPLAsm were produced following the procedure described by Orr, M. T., et al. (Orr et al., 2013).

Ovalbumin (OVA, 5 μg/dose) was used as an antigen. Female BALB/cAnNCri (Orientbio, ROK) mice (7 weeks old) were immunized via two intramuscular injections (0 and 14 days) with PBS alone, OVA (5 μg/dose) alone, EcML (5 μg/dose) alone, EcML (5 μg/dose) and OVA (5 μg/dose), GLA (5 μg/dose) and OVA (5 μg/dose), or MPLAsm (5 μg/dose) and OVA (5 μg/dose). Serum samples were collected 14 days after the second immunization. Each test group consisted of seven mice.

2.7. Analysis of antigen-specific antibodies

ELISA plates (SPL, ROK) were coated with OVA (Sigma-Aldrich) dissolved in carbonate buffer (BioLegend) overnight at 4 °C. The plates were then washed with PBST (0.05% Tween20 in PBS) and blocked with 1% bovine serum albumin dissolved in PBS buffer for 1 h at room temperature (RT). After washing the plates, 100 μL of 2-fold serial dilutions of serum were added to the wells, followed by incubation for 2 h at RT. After washing, the plates were incubated with HRP-conjugated goat anti-mouse IgG, IgG1, or IgG2a antibodies (Southern Biotech) for 2 h at RT. 3,3′,5,5′-tetramethylbenzidine (BioLegend) substrate (100 μL) was added to each well, and the plates were incubated for 10 min at RT. The reaction was terminated via addition of 2 N H_2SO_4 (50 μL per well). The absorbance values were read at 450 nm and were corrected for optical imperfections in the plates by subtracting absorbance values at 540 nm. Antibody titers were obtained by plotting the maximum serum dilution that gave an optical density > 5 × the background. The first serum dilution was started at 2^7 to analyze the IgG, IgG1, and IgG2a levels; therefore, the lowest titer for antibody was arbitrarily determined as 2^6.

Table 2
Mutation analyses of KHSC0003/pBAD33.1-lpxE$_{AA}$ genome via *de novo* sequencing in comparison with the published W3110 genome (Genbank accession number: AP009048) and that of the mother strain W3110 used for the strain construction.

Nucleotide position based on AP009048	W3110 (AP009048)	W3110 (mother strain)	KHSC0003/pBAD33.1-*lpxE*$_{AA}$
151,154	C	C	G (gly149ala mutation YadK)
547,694	A	G	G
547,831	AGGGG	AGGGGG	AGGGGG
556,858	A	T	T
1,065,700	C	T	T
1,093,686	T	C	C
1,097,580	C	T	T
1,117,836	C	C	C
1,303,712	A	G	G
2,019,202	C	T	T
2,906,975	C	G	G
4,371,270	GAAAAA	GAAA	GAAA
653,806–656,391	IS elements inserted in *dcuC*	Intact *ducC*	Intact *ducC*
656,979–657,539	*pagP*	*pagP*	Deleted
2,272,188–2,272,901	*lpxT*	*lpxT*	Deleted
3,830,597–3,831,875	*kdtA*	*kdtA*	Replaced with a kana-mycin resistance cassette

2.8. Statistical analysis

All of the data are presented as mean ± standard deviation (S.D.) for control and experimental samples. The sample size was chosen based on the most commonly used sizes in this area. Significance of differences comparing two groups was analyzed by two tailed unpaired student t-test. Statistical significances were set at $p < 0.05$; individual P values are indicated in figure legends.

3. Results and discussion

3.1. Metabolic engineering of E. coli for MPLA production

To develop a *de novo* biosynthetic pathway for MPLA production in *E. coli*, we engineered the strain according to the scheme shown in Fig. 3a. First, the genes encoding lipid A palmitoyltransferase and lipid A 1-diphosphate synthase (*pagP* (Bishop et al., 2000) and *lpxT* (Touze et al., 2008), respectively) were deleted from the *E. coli* chromosome to minimize potential side products (Fig. 2, purple-colored box, Fig. 3a). Second, a lipid A-producing strain was obtained by introducing a plasmid that co-overexpresses $LpxL_{EC}$ and $LpxM_{EC}$ followed by knocking out the gene encoding Kdo transferase ($kdtA_{EC}$ from the *E. coli* chromosome (Fig. 2, orange-colored box, Fig. 3a). While we were not able to obtain a colony by P1*vir* transduction carrying a *kdtA::kan* cassette into KHSC0001/pWSK29 within 48 h on a LB-agar plate at 30 °C, co-overexpression of $LpxL_{EC}$ and $LpxM_{EC}$ effectively suppresses the lethality of $kdtA_{EC}$ knockout, and the strain KHSC0003 survived and supported the efficient production of hexa-acylated lipid A. Thus, the resulting *E. coli* strain, KHSC0003 transformed with an empty pBAD33.1 vector (Table 1 and Fig. 3a), generated hexa-acylated lipid A species as one of its primary LPS molecules without the core oligosaccharide, as detected via thin-layer chromatography (TLC) (Fig. 3d, lane 1). Finally, to identify the appropriate LpxE enzymes that effectively dephosphorylate lipid A in *E. coli*, we cloned *lpxE* genes, including *Aquifex aeolicus* $lpxE_{AA}$ (locus tag: *aq_1706*) (Zhao et al., 2019), *Helicobacter pylori* $lpxE_{HP}$ (Tran et al., 2006) (locus tag: *hp0021*), *Francisella novicida* $lpxE_{FN}$ (locus tag: *ftn_0416*) (Wang et al., 2004), and *Rhizobium leguminosarum* $lpxE_{RL}$ (locus tag: *rl4708*) (Karbarz et al., 2003) in pBAD33.1 (Chung and Raetz, 2010) and transformed the constructs into KHSC0003 (Fig. 3a and b). Prior to this study, none of LpxE enzymes is known for the dephosphorylating activity of lipid A 1-phosphate in the absence of the Kdo_2 unit during LPS biosynthesis. Among the tested KHSC0003/pBAD33.1-*lpxEs*, KHSC0003/pBAD33.1-$lpxE_{AA}$ and KHSC0003/pBAD33.1-$lpxE_{HP}$ effectively produced MPLA assessed by TLC (Supplementary Fig. 3a).

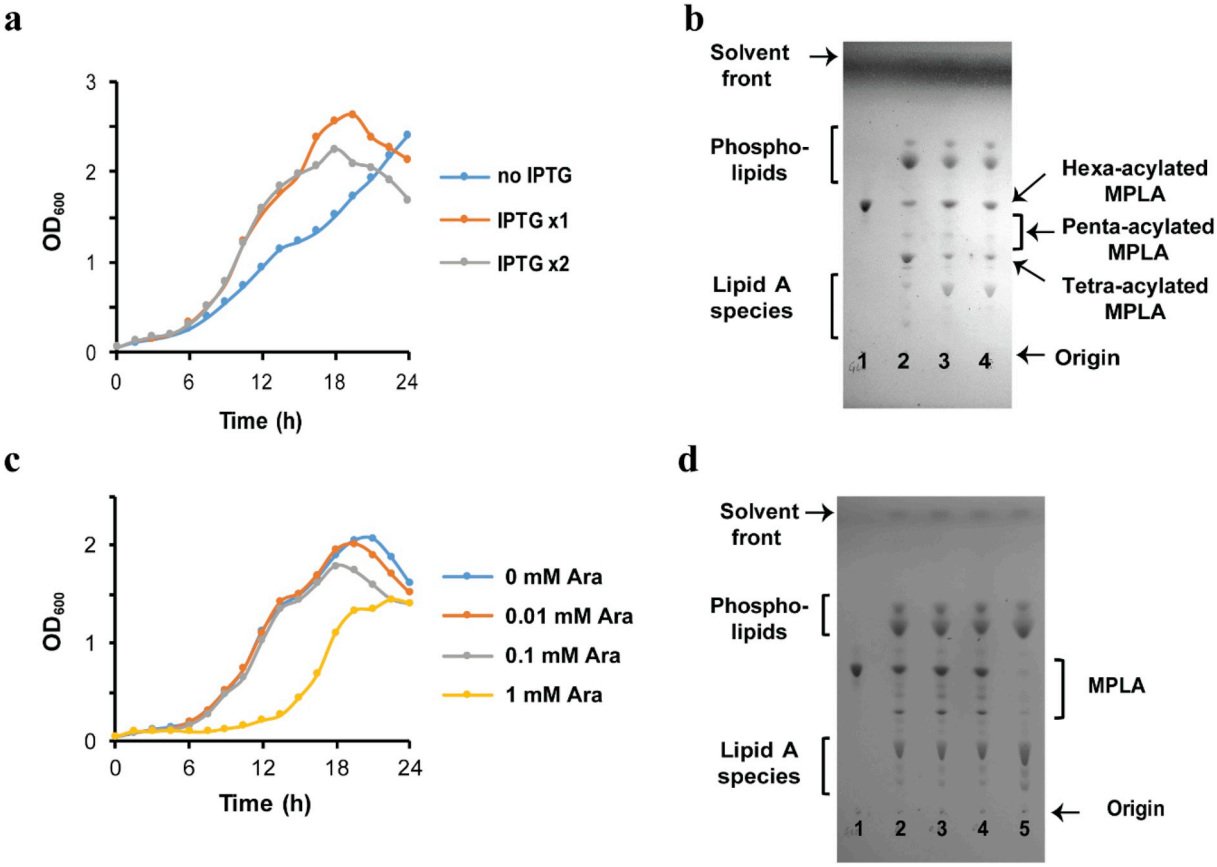

Fig. 4. Efficient production of hexa-acylated MPLA is achieved by overexpression of LpxL and LpxM along with leaky expression of LpxE. (a) Growth curves for KHSC0003/pBAD33.1-$lpxE_{AA}$ supplemented with or without IPTG. The strain was grown in LB medium containing ampicillin and chloramphenicol supplemented with 0 (no IPTG), 1 mM IPTG (IPTG 1x) at time 0 and 1 mM IPTG at time 0 and 12 h (IPTG 2x) after dilution. Overexpression of LpxL and LpxM increases the growth rate of the strain. (b) TLC profiles of the lipids extracted from the engineered *E. coli* strains compared with those of GLA (lane 1). Total lipids extracted from KHSC0003/pBAD33.1-$lpxE_{AA}$ cultured in the presence of 0 (lane 2), IPTG 1x (lane 3), and IPTG 2x (lane 4). Overexpression of LpxL and LpxM is required for efficient hexa-acylated MPLA production. (c) Growth curves for KHSC0003/pBAD33.1-$lpxE_{AA}$ supplemented with different concentrations of L-arabinose (Ara). The strain was grown in LB medium containing ampicillin, chloramphenicol, and IPTG supplemented with 0, 0.01, 0.1, 1 mM Ara. Overexpression of LpxE by 1 mM Ara caused a long lagging phase. (d) TLC profiles of the lipids extracted from the engineered *E. coli* strains compared with those of GLA (lane 1). Total lipids extracted from KHSC0003/pBAD33.1-$lpxE_{AA}$ cultured in the presence of 0 (lane 2), 0.01 mM Ara (lane 3), 0.1 mM Ara (lane 4), and 1 mM Ara (lane 5) at time 0. The presence of 1 mM Ara caused a long lagging phase of the strain growth, and the strain grown in the presence of 1 mM Ara barely produced MPLA. The presence of 0, 0.01, or 0.1 mM Ara does not affect MPLA production.

3.2. Characterization of a MPLA production strain, KHSC0003/pBAD33.1-lpxE$_{AA}$

In order to characterize strains along with the steps of metabolic engineering, we measured growth curves and calculated doubling times of the strains (Fig. 3c). As shown in Fig. 3c, *pagP* and *lpxT* double knockouts did not affect *E. coli* growth at 30 °C in LB medium compared to that of wild type W3110 (doubling time is about 44 min). However, the growth rate of KHSC0003 having a chromosomal *kdtA* knockout decreased to about 50% of that of W3110 (Fig. 3c), with a longer initial lag phase when the strain was cultured in LB medium supplemented with the addition of 1 mM IPTG at time 0 and 12 h. A longer initial lag phase was also observed in the ClearColi strain grown in LB, which lacks Kdo sugar biosynthetic pathway and has a suppressive mutation in *msbA* gene (Mamat et al., 2008), resulting in lipid IV$_A$ production instead of LPS (https://www.lucigen.com/docs/literature/eLucidations/ClearColi-Media-App-Note-April-2016.pdf). Growth rates of KHSC0003/pBAD33.1, KHSC0003/pBAD33.1-lpxE$_{AA}$, and KHSC0003/pBAD33.1-lpxE$_{HP}$ (doubling time: 122 ± 16, 144 ± 18, and 149 ± 14 min, respectively, Fig. 3c) decreased compared to that of

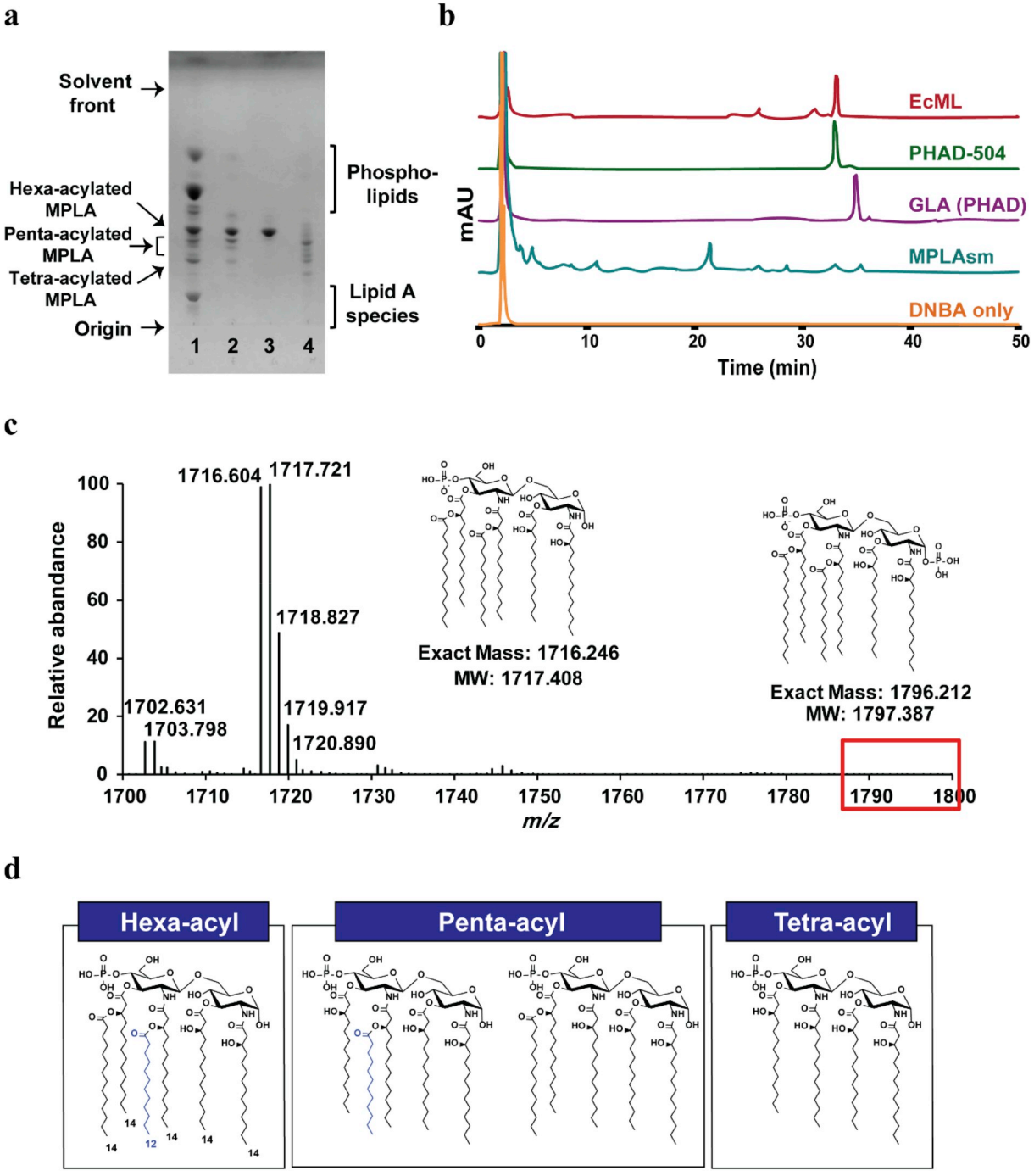

Fig. 5. Characterization of EcML purified from engineered *E. coli* KHSC0003/pBAD33.1-lpxE$_{AA}$ cells. (a) TLC profile of EcML (lane 2) purified from the total lipids of KHSC0003/pBAD33.1-lpxE$_{AA}$ (lane 1) compared to those of GLA (lane 3) and MPLAsm (lane 4). (b) The HPLC profile of EcML compared to those of DNBA, MPLAsm, GLA (PHAD), and PHAD-504. (c) The ESI-MS spectrum of EcML in the *m/z* range of 1700–1800 amu. Lipid A (calculated [M-H]$^-$: 1796.212), was not detected, while hexa-acylated MPLA (calculated [M-H]$^-$: 1716.246) was observed at 1716.604 by ESI-MS. (d) Suggested chemical structures of hexa-, penta-, and tetra-acylated EcML.

KHSC0003 (doubling time: 83 ± 11 min, Fig. 3c), probably due to the additional plasmid pBAD33.1 and leaky expression of LpxEs. OD_{600} values of KHSC0003 were gradually decreased at stationary phase indicating possible cell lysis.

Surprisingly, leaky $LpxE_{AA}$ or $LpxE_{HP}$ expression from pBAD33.1 led to dephosphorylation of the 1-phosphate group from hexa-, penta-, and tetra-acylated lipid A species and resulted in MPLA production, which was confirmed by performing TLC (Fig. 3d, lane 2 and 3, respectively) along with commercially available GLA (Fig. 3d, lane 4) and MPLAsm (Fig. 3d, lane 5) as standards. Since $LpxE_{AA}$ and $LpxE_{HP}$ produced similar amounts of MPLA in KHSC0003 and had similar growth rates, further characterization of the strain and MPLA production was done using the KHSC0003/pBAD33.1-*lpxE*$_{AA}$ strain. To analyze the genome sequence of KHSC0003/pBAD33.1-*lpxE*$_{AA}$, *de novo* sequencing was executed and compared to the published W3110 genome (Genbank accession number: AP009048) (Hayashi et al., 2006), Table 2). The identified SNPs and indels were compared to the corresponding sequence of W3110 used for the construction of KHSC0003/pBAD33.1-*lpxE*$_{AA}$ (Table 2). As seen in Table 2, the KHSC0003/pBAD33.1-*lpxE*$_{AA}$ strain has only one SNP, which is not originated from the mother strain at location 151,154 based on the nucleotide numbering of AP009048 genome. The C to G change at location 151,154 makes a 149th amino acid mutation of YadK (putative fimbrial-like protein) from glycine to alanine. Considering that the genomic location of *yadK* is too far to be transduced by P1*vir* during *pagP* (located at 656,979–657,539), *lpxT* (located at 2,272,188–2,272,901), or *kdtA* (located at 3,830,597–3,831,875) knockout process, this mutation is likely acquired spontaneously.

3.3. Evaluate the effects of LpxL, LpxM, and LpxE overexpression on the growth rate and MPLA production of KHSC0003/pBAD33.1-*lpxE*$_{AA}$

In order to optimize the strain growth and production of hexa-acylated MPLA that is suggested as the most potent adjuvant among MPLA congeners in human (Coler et al., 2011). We first checked the effect of LpxL and LpxM overexpression on the strain growth and MPLA production profile. In the absence of IPTG, we observed obvious decrease in the growth rate compared to that of the cultures supplemented with 1 mM IPTG at time 0 or time 0 and 12 h after dilution (Fig. 4a). As a note, while we did not add IPTG at the dilution point, there was IPTG carried over from the seeding culture. In addition, we observed the shift in the major congener composition of the MPLA from hexa-acylated to tetra-acylated MPLA depending on the LpxL and LpxM overexpression (Fig. 4b, lane 2 vs lane 3 and 4). Even though further experiments should be required to determine the optimum IPTG amounts, no obvious difference was observed in the growth rates (Fig. 3a) and MPLA composition assessed via TLC analysis (Fig. 4b, lane 3 vs lane 4) between the cultures supplemented with 1 mM IPTG at time 0 or time 0 and 12 h after dilution. Therefore 1 mM IPTG would be sufficient for hexa-acylated MPLA production. In order to increase MPLA formation relative to lipid A species, we overexpressed LpxE with different concentrations of arabinose. Unexpectedly, the culture grown with 1 mM arabinose had a long lagging phase (about 10 h) before starting growth (Fig. 4c) and dramatically reduced the amount of MPLA production (Fig. 4d, lane 5) compared to those of the cultures supplemented with 0, 0.01, or 0.1 mM arabinose (Fig, 4d, lane 2, 3, and 4, respectively). Such a result indicated that overexpression of LpxE with 1 mM arabinose might be toxic to the strain, generating spontaneously mutanted strains, in which LpxE could not function properly. The cultures supplemented with 0, 0.01, or 0.1 mM arabinose showed similar growth rates, and the MPLA production profiles assessed by TLC analysis indicated that leaky expression of LpxE from the pBAD33.1 plasmid is the best growth condition for MPLA production to mitigate the risk of mutants' selection. At this point, it is not clear why the *kdtA* knockout with overexpression of LpxL and LpxM showed gradual lysis phenotype at the stationary phase (Figs. 3c, 4a and 4c) and it would be an interesting research topic to understand the outer membrane biogenesis of the final strain to enhance biomass.

3.4. Characterization of total lipids and purified MPLA, EcML

Matrix-assisted laser desorption ionization-time of flight mass spectrometry (MALDI-TOF MS) analysis of the total lipids extracted from KHSC0003/pBAD33.1-*lpxE*$_{AA}$ cells confirmed the presence of hexa-acylated MPLA ($[M-H]^-$ of hexa-acylated MPLA: calculated = 1716.246 and observed = 1716.305, Supplementary Fig. 4). Based on the TLC (Fig. 5a, lane 1) and MALDI-TOF (Supplementary Fig. 4) data, the KHSC0003/pBAD33.1-*lpxE*$_{AA}$ total lipid extract contained lipid A (calculated $[M-H]^-$ = 1796.212 and observed $[M-H]^-$ = 1796.270) (~40–50% of the total LPS species), and MPLA. To allow the MPLA produced by the engineered *E. coli* strains to be safely used as an adjuvant, we removed lipid A by taking advantage of the negative charge difference between MPLA (mono-phosphorylated species) and lipid A (bis-phosphorylated species). After purification of the MPLA via anion-exchange chromatography (DE52 resin, Biophoretics) (Fig. 5a, lane 2), we named the purified MPLA "*E. coli*-derived monophosphoryl lipid A (EcML)". EcML was purified at a yield of 8–12 mg/1 L of LB and 13–19 mg/g dry cell weight (DCW) (Table 3). The purity and lipid A contamination of EcML were also assessed via TLC with increasing amounts of EcML (Supplementary Fig. 5) and electrospray ionization-mass spectrometry (ESI-MS) (Fig. 5c and Supplementary Fig. 6), both of which showed no lipid A carry-over (Fig. 5c, red box). Using the ImageJ program (Schneider et al., 2012), we determined the purities of EcML, GLA, and MPLAsm as 80–89% (depending on the different batches), 90%, and 88%, respectively based on the TLC images shown in Figs. 3d and 5a, and Supplementary Fig. 5. Majority of impurities are phospholipids (Fig. 5a). Considering that each Cervarix dose contains 50 μg of MPL, about 10 mg of EcML would be sufficient to generate 200 doses. Although EcML contained more of a complex mixture of hexa-, penta-, and tetra-acylated MPLA (Fig. 5a, lane 2) than GLA (Fig. 5a, lane 3), its composition was simpler than that of MPLAsm (Fig. 5a, lane 4). To determine the relative distribution of hexa-, penta-, and tetra-acylated MPLA and batch variation of EcML, three different batches of EcML, MPLAsyn (GLA and PHAD-504), and MPLAsm were modified with dinitrobenzyloxyamine hydrochloride (DNBA) according to a previously described procedure (Hagen et al., 1997) and analyzed via high-performance liquid chromatography (HPLC) (Fig. 5b and Supplementary Fig. 7). Since $LpxL_{EC}$ preferentially transfers a lauroyl group during LPS and MPLA biosynthesis in *E. coli* (Fig. 2), the major hexa-acylated EcML (Fig. 5d) component has the same chemical structure as PHAD-504 (Fig. 1c, right), resulting in the same retention time as shown in HPLC profiles (Fig. 5b). EcML contained about 69.7% ± 3.8% of hexa-, 22.2% ± 3.3% of penta-, and 8.2% ± 0.7% of tetra-acylated MPLA (Table 3, the predicted chemical structures of hexa-, penta-, tetra-acylated MPLA are shown in Fig. 5d). Furthermore, our results demonstrated that the congener compositions of EcML from different batches are fairly consistent (Table 3 and Supplementary Fig. 7). It is worth noting that the HPLC analyses of MPLAsm from two different vendors, Invivogen and Avanti Polar Lipids, showed large variations in their

Table 3
Batch-to-batch variations in EcML yield and congener composition.

	Batch	Yield mg/25g LB (mg/g DCW[a])	Composition (%): number of acyl chain		
			Hexa	Penta	Tetra
EcML	1	8.4 (12.7)	68.5	23.7	7.9
	2	12.4 (18.6)	66.6	24.5	9.0
	3	8.4 (13.9)	73.9	18.5	7.6
Average ± STD		**9.7 ± 2.3 (14.7 ± 3.3)**	**69.7 ± 3.8**	**22.2 ± 3.3**	**8.2 ± 0.7**

[a] DCW of KHSC0003/pBAD33.1-*lpxE*$_{AA}$ is 0.29 g for 1L of OD_{600} = 1.0.

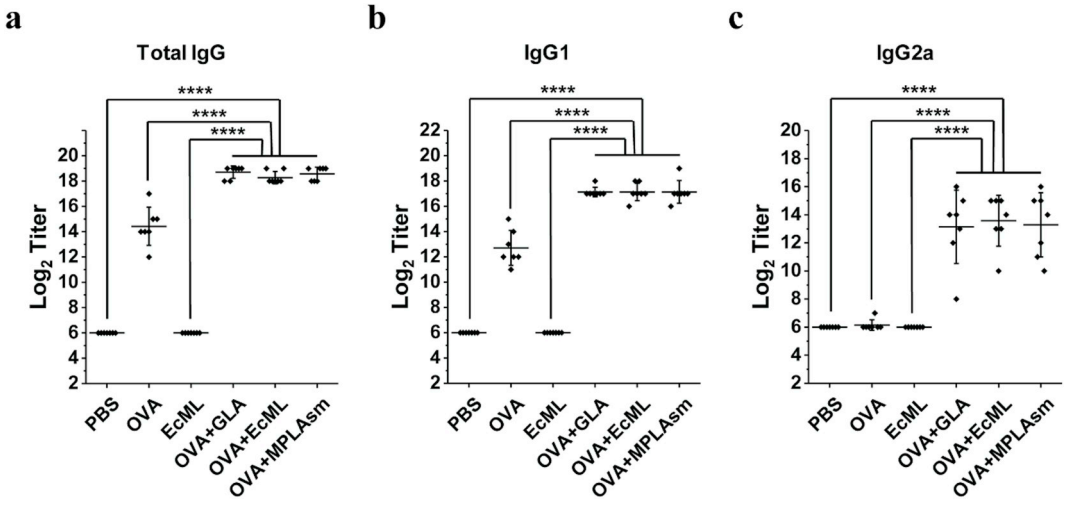

Fig. 6. Evaluation of antigen (ovalbumin, OVA)-specific antibody responses show that EcML has equal adjuvanticity to those of GLA and MPLAsm (Invivogen). Total IgG, IgG1, and IgG2a antibody titers measured 14 days after the second immunization with PBS only, OVA only, EcML only, OVA together with GLA, OVA together with EcML, or OVA together with MPLAsm. (a) Total IgG endpoint titers, (b) IgG1 endpoint titers, and (c) IgG2a endpoint titers. Data are presented as mean ± S.D. (n = 7; ****$p < 0.0001$; two-tailed unpaired student t-test). The lowest antibody titer was arbitrarily determined as 2^6, as the first sample tested was a 2^7 dilution of the serum. Error bars represent the standard deviations.

congener compositions due to uncontrollable aspects of the acid/base hydrolysis process (Supplementary Fig. 8), which significantly complicates the MPLAsm quality control. Accordingly, the simplicity and low batch-to-batch variations in congener composition intrinsic to our EcML preparation method offer particular advantages for its use in chemistry, manufacturing, and controls for clinical trials or marketing applications.

3.5. EcML effectively enhances antigen-specific antibody formation in mice model

After characterization of the prepared EcML, we determined its adjuvanticity. Aqueous formulations of EcML, along with MPLAsm and GLA as positive controls, were produced according to a published procedure (Orr et al., 2013). As shown in Fig. 6, EcML potentiated antigen-specific IgG, IgG1, and IgG2a production to a similar extent as the positive controls in BALB/c mice when ovalbumin was used as an antigen. Taken together, these results strongly suggest that the adjuvanticity of EcML purified from the engineered *E. coli* strain is equal to those of commercially available GLA and MPLAsm for antigen-specific antibody formation after vaccination.

4. Conclusion

Over the course of the rapid growth of the vaccine and immunotherapy markets, MPLA has played pivotal roles in the development of vaccines and immunotherapy for allergies, cancer, and Alzheimer's disease. However, the production methods for GLA and MPLAsm suffer from complexity in synthetic steps and quality control, respectively, and the production costs are high for both methods. The MPLA-producing *E. coli* strain would be a succinct, cost-effective, and sustainable resource to meet the increasing demand of MPLA not only as an adjuvant but also as emerging therapeutic options for humans and animals.

Acknowledgements

We thank Robert A. Gillespie for providing pET28b-*lpxE*$_{AA}$.

Appendix A. Supplementary data

Supplementary data to this article can be found online at https://doi.org/10.1016/j.ymben.2019.11.009.

Funding information

This work was supported by KIST intramural grants, by the Pioneer Research Center Program (2014M3C1A3054141) through the National Research Foundation of Korea funded by the Ministry of Science, ICT and Future Planning, by the Ministry of Trade, Industry & Energy (MOTIE), Korea Institute for Advancement of Technology(KIAT) through the Encouragement Program for The Industries of Economic Cooperation Region (P0006222), and by the National Institute of General Medical Sciences, USA (GM115355 to PZ). The funders had no role in study design, data collection and interpretation, or the decision to submit the work for publication.

References

Baba, T., Ara, T., Hasegawa, M., Takai, Y., Okumura, Y., Baba, M., Datsenko, K.A., Tomita, M., Wanner, B.L., Mori, H., 2006. Construction of *Escherichia coli* K-12 in-frame, single-gene knockout mutants: the Keio collection. Mol. Syst. Biol. 2 2006 0008.

Bishop, R.E., Gibbons, H.S., Guina, T., Trent, M.S., Miller, S.I., Raetz, C.R., 2000. Transfer of palmitate from phospholipids to lipid A in outer membranes of gram-negative bacteria. EMBO J. 19 (19), 5071–5080.

Bligh, E.G., Dyer, W.J., 1959. A rapid method of total lipid extraction and purification. Can. J. Biochem. Physiol. 37 (8), 911–917.

Casella, C.R., Mitchell, T.C., 2008. Putting endotoxin to work for us: monophosphoryl lipid A as a safe and effective vaccine adjuvant. Cell. Mol. Life Sci. 65 (20), 3231–3240.

Chung, H.S., Raetz, C.R., 2010. Interchangeable domains in the Kdo transferases of *Escherichia coli* and *Haemophilus influenzae*. Biochemistry 49 (19), 4126–4137.

Coler, R.N., Bertholet, S., Moutaftsi, M., Guderian, J.A., Windish, H.P., Baldwin, S.L., Laughlin, E.M., Duthie, M.S., Fox, C.B., Carter, D., Friede, M., Vedvick, T.S., Reed, S.G., 2011. Development and characterization of synthetic glucopyranosyl lipid adjuvant system as a vaccine adjuvant. PLoS One 6 (1).

Datsenko, K.A., Wanner, B.L., 2000. One-step inactivation of chromosomal genes in *Escherichia coli* K-12 using PCR products. Proc. Natl. Acad. Sci. U. S. A 97 (12), 6640–6645.

Grant, S.G., Jessee, J., Bloom, F.R., Hanahan, D., 1990. Differential plasmid rescue from transgenic mouse DNAs into *Escherichia coli* methylation-restriction mutants. Proc. Natl. Acad. Sci. U. S. A 87 (12), 4645–4649.

Hagar, J.A., Powell, D.A., Aachoui, Y., Ernst, R.K., Miao, E.A., 2013. Cytoplasmic LPS activates caspase-11: implications in TLR4-independent endotoxic shock. Science 341 (6151), 1250–1253.

Hagen, S.R., Thompson, J.D., Snyder, D.S., Myers, K.R., 1997. Analysis of a

monophosphoryl lipid A immunostimulant preparation from *Salmonella minnesota* R595 by high-performance liquid chromatography. J. Chromatogr. A 767 (1–2), 53–61.
Hayashi, K., Morooka, N., Yamamoto, Y., Fujita, K., Isono, K., Choi, S., Ohtsubo, E., Baba, T., Wanner, B.L., Mori, H., Horiuchi, T., 2006. Highly accurate genome sequences of *Escherichia coli* K-12 strains MG1655 and W3110. Mol. Syst. Biol. 2 2006 0007.
Karbarz, M.J., Kalb, S.R., Cotter, R.J., Raetz, C.R., 2003. Expression cloning and biochemical characterization of a *Rhizobium leguminosarum* lipid A 1-phosphatase. J. Biol. Chem. 278 (41), 39269–39279.
Karbarz, M.J., Six, D.A., Raetz, C.R., 2009. Purification and characterization of the lipid A 1-phosphatase LpxE of *Rhizobium leguminosarum*. J. Biol. Chem. 284 (1), 414–425.
Kayagaki, N., Wong, M.T., Stowe, I.B., Ramani, S.R., Gonzalez, L.C., Akashi-Takamura, S., Miyake, K., Zhang, J., Lee, W.P., Muszynski, A., Forsberg, L.S., Carlson, R.W., Dixit, V.M., 2013. Noncanonical inflammasome activation by intracellular LPS independent of TLR4. Science 341 (6151), 1246–1249.
Lu, Y.C., Yeh, W.C., Ohashi, P.S., 2008. LPS/TLR4 signal transduction pathway. Cytokine 42 (2), 145–151.
Lu, Y.H., Guan, Z., Zhao, J., Raetz, C.R., 2011. Three phosphatidylglycerol-phosphate phosphatases in the inner membrane of *Escherichia coli*. J. Biol. Chem. 286 (7), 5506–5518.
Mamat, U., Meredith, T.C., Aggarwal, P., Kuhl, A., Kirchhoff, P., Lindner, B., Hanuszkiewicz, A., Sun, J., Holst, O., Woodard, R.W., 2008. Single amino acid substitutions in either YhjD or MsbA confer viability to 3-deoxy-d-manno-oct-2-ulosonic acid-depleted *Escherichia coli*. Mol. Microbiol. 67 (3), 633–648.
Michaud, J.P., Halle, M., Lampron, A., Theriault, P., Prefontaine, P., Filali, M., Tribout-Jover, P., Lanteigne, A.M., Jodoin, R., Cluff, C., Brichard, V., Palmantier, R., Pilorget, A., Larocque, D., Rivest, S., 2013. Toll-like receptor 4 stimulation with the detoxified ligand monophosphoryl lipid A improves Alzheimer's disease-related pathology. Proc. Natl. Acad. Sci. U. S. A 110 (5), 1941–1946.
Miroux, B., Walker, J.E., 1996. Over-production of proteins in *Escherichia coli*: mutant hosts that allow synthesis of some membrane proteins and globular proteins at high levels. J. Mol. Biol. 260 (3), 289–298.
Orr, M.T., Fox, C.B., Baldwin, S.L., Sivananthan, S.J., Lucas, E., Lin, S., Phan, T., Moon, J.J., Vedvick, T.S., Reed, S.G., Coler, R.N., 2013. Adjuvant formulation structure and composition are critical for the development of an effective vaccine against *tuberculosis*. J. Control. Release 172 (1), 190–200.
Paya Cuenca, C.V.S.F., Ter Meulen, Jan Henrik, 2015. GLA Monotherapy for Use in Cancer Treatment, United States Patent. CA, US. Immune Design Corp., (Seattle, WA, US), United States Mercer Island, WA, US.
Poltorak, A., He, X., Smirnova, I., Liu, M.Y., Van Huffel, C., Du, X., Birdwell, D., Alejos, E., Silva, M., Galanos, C., Freudenberg, M., Ricciardi-Castagnoli, P., Layton, B., Beutler, B., 1998. Defective LPS signaling in C3H/HeJ and C57BL/10ScCr mice: mutations in Tlr4 gene. Science 282 (5396), 2085–2088.
Qureshi, N., Takayama, K., Ribi, E., 1982. Purification and structural determination of nontoxic lipid A obtained from the lipopolysaccharide of *Salmonella typhimurium*. J. Biol. Chem. 257 (19), 11808–11815.
Raetz, C.R., Whitfield, C., 2002. Lipopolysaccharide endotoxins. Ann. Rev. Biochem. 71, 635–700.
Raetz, C.R., Purcell, S., Meyer, M.V., Qureshi, N., Takayama, K., 1985. Isolation and characterization of eight lipid A precursors from a 3-deoxy-D-manno-octylosonic acid-deficient mutant of *Salmonella typhimurium*. J. Biol. Chem. 260 (30), 16080–16088.
Reed, S.G., Hsu, F.C., Carter, D., Orr, M.T., 2016. The science of vaccine adjuvants: advances in TLR4 ligand adjuvants. Curr. Opin. Immunol. 41, 85–90.
Reed, S.G., Carter, D., 2014. Synthetic Glucopyranosyl lipid adjuvants. In: United States Patent. Infectious Disease Research Institute, US.
Reed, S.G., Carter, D., Casper, C., Duthie, M.S., Fox, C.B., 2018. Correlates of GLA family adjuvants' activities. Semin. Immunol. 39, 22–29.
Schneider, C.A., Rasband, W.S., Eliceiri, K.W., 2012. NIH Image to ImageJ: 25 years of image analysis. Nat. Methods 9 (7), 671–675.
Seidman, C.E., Struhl, K., Sheen, J., Jessen, J., 1997. Introduction of plasmid DNA into cells. Curr. Protoc. Mol. Biol. 1.8.1–1.8.10.
Shi, J., Zhao, Y., Wang, Y., Gao, W., Ding, J., Li, P., Hu, L., Shao, F., 2014. Inflammatory caspases are innate immune receptors for intracellular LPS. Nature 514 (7521), 187–192.
Thomason, L.C., Costantino, N., Court, D.L., coli, E., 2007. Genome maniplation by P1 transduction. Curr. Protoc. Mol. Biol. 1.17.1–1.17.8. https://doi.org/10.1002/0471142727.mb0117s79.
Touze, T., Tran, A.X., Hankins, J.V., Mengin-Lecreulx, D., Trent, M.S., 2008. Periplasmic phosphorylation of lipid A is linked to the synthesis of undecaprenyl phosphate. Mol. Microbiol. 67 (2), 264–277.
Tran, A.X., Whittimore, J.D., Wyrick, P.B., McGrath, S.C., Cotter, R.J., Trent, M.S., 2006. The lipid A 1-phosphatase of *Helicobacter pylori* is required for resistance to the antimicrobial peptide polymyxin. J. Bacteriol. 188 (12), 4531–4541.
Wang, R.F., Kushner, S.R., 1991. Construction of versatile low-copy-number vectors for cloning, sequencing and gene expression in *Escherichia coli*. Gene 100, 195–199.
Wang, X., Karbarz, M.J., McGrath, S.C., Cotter, R.J., Raetz, C.R., 2004. MsbA transporter-dependent lipid A 1-dephosphorylation on the periplasmic surface of the inner membrane: topography of *Francisella novicida* LpxE expressed in *Escherichia coli*. J. Biol. Chem. 279 (47), 49470–49478.
Wang, B., Han, Y., Li, Y., Li, Y., Wang, X., 2015. Immuno-stimulatory activity of *Escherichia coli* mutants producing Kdo_2-monophosphoryl-lipid A or Kdo_2-pentaacyl-monophosphoryl-lipid A. PLoS One 10 (12), e0144714.
Zhao, J., An, J., Hwang, D., Wu, Q., Wang, S., Gillespie, R.A., Yang, E.G., Guan, Z., Zhou, P., Chung, H.S., 2019. The lipid A 1-phosphatase, LpxE, functionally connects multiple layers of bacterial envelope biogenesis. mBio 10 (3). https://doi.org/10.1128/mBio.00886-19.